ARTICLES

Measurement of the inclusive semielectronic D^0 branching fraction

Y. Kubota, M. Lattery, J. K. Nelson, S. Patton, R. Poling, T. Riehle, V. Savinov, and R. Wang
University of Minnesota, Minneapolis, Minnesota 55455

M. S. Alam, I. J. Kim, Z. Ling, A. H. Mahmood, J. J. O'Neill, H. Severini, C. R. Sun, S. Timm, and F. Wappler
State University of New York at Albany, Albany, New York 12222

G. Crawford, J. E. Duboscq, R. Fulton, D. Fujino, K. K. Gan, K. Honscheid, H. Kagan, R. Kass, J. Lee, M. Sung, C. White, R. Wanke, A. Wolf, and M. M. Zoeller
Ohio State University, Columbus, Ohio 43210

X. Fu, B. Nemati, W. R. Ross, P. Skubic, and M. Wood
University of Oklahoma, Norman, Oklahoma 73019

M. Bishai, J. Fast, E. Gerndt, J. W. Hinson, T. Miao, D. H. Miller, M. Modesitt, E. I. Shibata, I. P. J. Shipsey, and P. N. Wang
Purdue University, West Lafayette, Indiana 47907

L. Gibbons, S. D. Johnson, Y. Kwon, S. Roberts, and E. H. Thorndike
University of Rochester, Rochester, New York 14627

T. E. Coan, J. Dominick, V. Fadeyev, I. Korolkov, M. Lambrecht, S. Sanghera, V. Shelkov, R. Stroynowski, I. Volobouev, and G. Wei
Southern Methodist University, Dallas, Texas 75275

M. Artuso, M. Gao, M. Goldberg, D. He, N. Horwitz, S. Kopp, G. C. Moneti, R. Mountain, F. Muheim, Y. Mukhin, S. Playfer, T. Skwarnicki, S. Stone, and X. Xing
Syracuse University, Syracuse, New York 13244

J. Bartelt, S. E. Csorna, V. Jain, and S. Marka
Vanderbilt University, Nashville, Tennessee 37235

D. Gibaut, K. Kinoshita, P. Pomianowski, and S. Schrenk
Virginia Polytechnic Institute and State University, Blacksburg, Virginia 24061

B. Barish, M. Chadha, S. Chan, D. F. Cowen, G. Eigen, J. S. Miller, C. O'Grady, J. Urheim, A. J. Weinstein, and F. Würthwein
California Institute of Technology, Pasadena, California 91125

D. M. Asner, M. Athanas, D. W. Bliss, W. S. Brower, G. Masek, and H. P. Paar
University of California, San Diego, La Jolla, California 92093

0556-2821/96/54(5)/2994(12)/$10.00

J. Gronberg, C. M. Korte, R. Kutschke, S. Menary, R. J. Morrison, S. Nakanishi, H. N. Nelson, T. K. Nelson, C. Qiao, J. D. Richman, D. Roberts, A. Ryd, H. Tajima, and M. S. Witherell
University of California, Santa Barbara, California 93106

R. Balest, K. Cho, W. T. Ford, M. Lohner, H. Park, P. Rankin, J. Roy, and J. G. Smith
University of Colorado, Boulder, Colorado 80309-0390

J. P. Alexander, C. Bebek, B. E. Berger, K. Berkelman, K. Bloom, T. E. Browder,* D. G. Cassel, H. A. Cho, D. M. Coffman, D. S. Crowcroft, M. Dickson, P. S. Drell, D. J. Dumas, R. Ehrlich, R. Elia, P. Gaidarev, B. Gittelman, S. W. Gray, D. L. Hartill, B. K. Heltsley, S. Henderson, C. D. Jones, S. L. Jones, J. Kandaswamy, N. Katayama, P. C. Kim, D. L. Kreinick, T. Lee, Y. Liu, G. S. Ludwig, J. Masui, J. Mevissen, N. B. Mistry, C. R. Ng, E. Nordberg, J. R. Patterson, D. Peterson, D. Riley, A. Soffer, and C. Ward
Cornell University, Ithaca, New York 14853

P. Avery, A. Freyberger, K. Lingel, C. Prescott, J. Rodriguez, S. Yang, and J. Yelton
University of Florida, Gainesville, Florida 32611

G. Brandenburg, D. Cinabro, T. Liu, M. Saulnier, R. Wilson, and H. Yamamoto
Harvard University, Cambridge, Massachusetts 02138

T. Bergfeld, B. I. Eisenstein, J. Ernst, G. E. Gladding, G. D. Gollin, M. Palmer, M. Selen, and J. J. Thaler
University of Illinois, Champaign-Urbana, Illinois 61801

K. W. Edwards, K. W. McLean, and M. Ogg
Carleton University and the Institute of Particle Physics, Ottawa, Ontario K1S 5B6, Canada

A. Bellerive, D. I. Britton, E. R. F. Hyatt, R. Janicek, D. B. MacFarlane, P. M. Patel, and B. Spaan
McGill University and the Institute of Particle Physics, Montréal, Québec H3A 2T8, Canada

A. J. Sadoff
Ithaca College, Ithaca, New York 14850

R. Ammar, P. Baringer, A. Bean, D. Besson, D. Coppage, N. Copty, R. Davis, N. Hancock, S. Kotov, I. Kravchenko, and N. Kwak
University of Kansas, Lawrence, Kansas 66045

(CLEO Collaboration)

(Received 25 October 1995)

Using the angular correlation between the π^+ emitted in a $D^{*+}\to D^0\pi^+$ decay and the e^+ emitted in the subsequent $D^0\to Xe^+\nu$ decay, we have measured the branching fraction for the inclusive semielectronic decay of the D^0 meson to be $\mathcal{B}(D^0\to Xe^+\nu)=[6.64\pm0.18(\text{stat})\pm0.29(\text{syst})]\%$. The measurement uses 1.7 fb^{-1} of e^+e^- collisions recorded by the CLEO II detector located at the Cornell Electron Storage Ring (CESR). Combining this result with previous CLEO results we find $\mathcal{B}(D^0\to Xe^+\nu)/\mathcal{B}(D^0\to K^-\pi^+)=1.684\pm0.056(\text{stat})\pm0.093(\text{syst})$ and $\mathcal{B}(D^0\to K^-e^+\nu)/\mathcal{B}(D^0\to Xe^+\nu)=0.581\pm0.023(\text{stat})\pm0.028(\text{syst})$. The difference between this inclusive rate and the sum of the measured exclusive branching fractions (measured at CLEO and other experiments) is also presented. [S0556-2821(96)02217-5]

PACS number(s): 13.20.Fc, 14.40.Lb

I. INTRODUCTION

Recent experimental measurements of the exclusive semileptonic branching fractions of the D^0 meson have yielded precise measurements of the dominant Cabibbo-favored modes, observation and measurement of the Cabibbo-suppressed branching fractions, and stringent upper limits on other Cabibbo-favored branching fractions. A comparison of the sum of these observed exclusive semileptonic branching fractions with the measured inclusive semileptonic branching fraction provides a measure of *missing* or unobserved modes. However, a new measurement of the inclusive semileptonic branching fraction is necessary to match the precision of the exclusive measurements. In this paper, the CLEO Collaboration presents an improved measurement of the inclusive semielectronic branching fraction of the D^0 meson. We then compare this inclusive measurement to the sum of the observed exclusive branching fractions measured at CLEO and other experiments.

*Permanent address: University of Hawaii at Manoa.

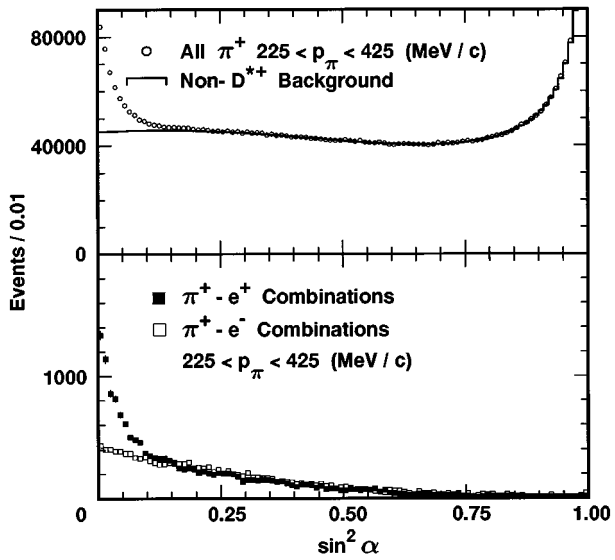

FIG. 1. The inclusive $\sin^2\alpha$ distribution for candidate pions (open circles) and the derived non-D^{*+} background (solid line) in the top plot. Requiring an electron near the pion with the same (opposite) sign results in the solid (open) squares in the bottom plot.

In addition, we combine our inclusive measurement with previous CLEO results on $\mathcal{B}(D^0\to K^-\pi)$ and $\mathcal{B}(D^0\to K^-e^+\nu)/\mathcal{B}(D^0\to K^-\pi^+)$ [3,4] to obtain the ratio $\mathcal{B}(D^0\to K^-e^+\nu)/\mathcal{B}(D^0\to Xe^+\nu)$. As a check of the analysis method, the observed inclusive electron momentum spectrum is also extracted from the data and compared with a Monte Carlo simulation. For a complete review of experimental and theoretical developments we refer the reader to recent reviews [1,2].

II. ANALYSIS TECHNIQUE AND EVENT SELECTION

The technique used to measure the absolute inclusive semielectronic branching fraction of D^0 mesons is similar to that used in the CLEO measurement of $\mathcal{B}(D^0\to K^-\pi^+)$ [3]. Both analyses must determine the number of $D^{*+}\to D^0\pi^+$ decays in the data and this is done using the following technique. The topology of $e^+e^-\to c\bar{c}$ reactions at a center of mass energy of 10.5 GeV requires the thrust axis (the axis along which the sum of the projected track and shower momenta is a maximum) for the event to approximate the D^{*+} direction in the laboratory. Limited available phase space in the $D^{*+}\to D^0\pi^+$ decay results in a small angle, denoted as α, between the thrust axis and the charged pion. Also, the magnitude of the pion momentum is correlated to the parent D^{*+} momentum. It is kinematically forbidden that pions with momentum greater than 225 MeV/c come from the $\Upsilon(4S)\to B\bar{B}$, $B\to D^{*+}X$, $D^{*+}\to D^0\pi^+$ decay chain. Selecting higher momentum pions ensures that the parent D^{*+} is produced via $e^+e^-\to c\bar{c}$ production, and that the thrust axis is correlated with the D^{*+} direction. The top plot in Fig. 1 shows the $\sin^2\alpha$ distribution for all pions with momentum between 225 and 425 MeV/c in the data. The peaking of the distribution at low $\sin^2\alpha$ is evidence for $D^{*+}\to D^0\pi^+$ decays. The total number of decays in the sample is $N(D^{*+}\to D^0\pi^+)=165\,658\pm1149(\text{stat})\pm2485(\text{syst})$, identical to Ref. [3], as the same data and selection criteria have been used in both analyses. See Ref. [3] for a discussion of the systematic error on this number and for a discussion of how the signal and background shapes are modeled.

To determine the total number of semielectronic decays, $N(D^{*+}\to D^0\pi^+,\ D^0\to Xe^+\nu)$, in this sample, an e^+ is sought within a cone around the π^+ direction. If found, the value of $\sin^2\alpha$ for its associated π^+ is plotted. ''Right-sign'' charge combinations π^+e^+ provide the signal distribution and ''wrong-sign'' combinations π^+e^- are studied to determine the background. Once the number of $D^0\to Xe^+\nu$ decays has been extracted, the branching fraction is then

$$\mathcal{B}(D^0\to Xe^+\nu)=\frac{N(D^{*+}\to D^0\pi^+,D^0\to Xe^+\nu)}{N(D^{*+}\to D^0\pi^+)\times\epsilon(D^0\to Xe^+\nu)}, \tag{1}$$

where $\epsilon(D^0\to Xe^+\nu)$ is the efficiency for detecting the electron.

A detailed description of the CLEO II detector can be found in Ref. [5]. Electrons [6] are identified principally from the ratio of the energy measured by the CsI calorimeter and the momentum measured by the drift chamber (E/p). Additional information on energy loss in the drift chamber and shower shape in the calorimeter is also used. Requiring momentum greater than 0.7 GeV/c and a polar angle with respect to the beam axis (θ) between 45° and 135° helps ensure a well-determined electron identification efficiency, with minimal uncertainty due to misidentified hadronic tracks. Furthermore, the number of electrons from $D^0\to X\pi^0$, $\pi^0\to e^+e^-\gamma$, where the $e^+e^-\gamma$ final state is due to either a Dalitz decay of the π^0 or a γ conversion in the detector material, should be suppressed. This is accomplished by requiring that the identified electron, when combined with each oppositely charged track (potentially an unidentified positron) in the event, does not yield an electron-positron mass below 0.050 GeV/c^2.

In order to correlate the electron with its associated charged pion, a fiducial angle cut is applied in the laboratory frame; we require that $\cos(\Theta_{e\text{-}\pi})>0.8$, where $\Theta_{e\text{-}\pi}$ is the angle between the charged pion and the electron. The bottom histogram in Fig. 1 shows the $\sin^2\alpha$ distributions for charged pions after requiring an electron within this angular region; the solid squares are for π^+e^+ combinations (right sign) and the open squares are for π^+e^- combinations (wrong sign).

III. EXTRACTION OF YIELDS

As previously stated, the yield of $D^{*+}\to D^0\pi^+$ decays is identical to that presented in Ref. [3]. In this section we detail the determination of the number of $D^0\to Xe^+\nu$ decays associated with the initial $D^{*+}\to D^0\pi^+$ decay.

The $\sin^2\alpha$ distribution for π^+e^+ (right-sign) combinations contains three distinct components: signal and two types of background. One background has a $\sin^2\alpha$ distribution that is identical to the signal as it originates from the decay $D^{*+}\to D^0\pi^+$, $D^0\to X\mathcal{F}_{e^+}$, where $\mathcal{F}_{e^+}$ denotes either a hadronic track misidentified as an electron or an electron from a $\pi^0\to e^+e^-\gamma$ final state. The other background is due to random soft pions (225–425 MeV/c in momentum) in coincidence with an electron, and is not as sharply peaked

near $\sin^2\alpha=0$ as the signal distribution.

The $\sin^2\alpha$ distribution for π^+e^- (wrong-sign) combinations is devoid of signal but contains the same two sources of background as the right-sign distribution [7]. It will be shown that the normalizations for these two backgrounds differ between the right-sign and wrong-sign distributions, although the shapes are identical.

The right-sign and wrong-sign distributions are fit simultaneously using the functional forms

$$\mathcal{G}^i_{\rm RS}(\sin^2\alpha)=N^i_{\rm RS}[D^0\to Xe^+\nu \ \text{ or } \ D^0\to X\mathcal{F}_e]g^i(\sin^2\alpha) + B^i_{\rm RS}P^i_2(\sin^2\alpha), \tag{2}$$

$$\mathcal{G}^i_{\rm WS}(\sin^2\alpha)=b^i_{\rm WS}[D^0\to X\mathcal{F}_e]g^i(\sin^2\alpha)+B^i_{\rm WS}P^i_2(\sin^2\alpha). \tag{3}$$

A Monte Carlo simulation determines the expected distributions $g^i(\sin^2\alpha)$, where i denotes the π momentum bin. This simulation correctly reproduces the measured D^{*+} production momentum distribution, and simulates $D^0\to Xe^+\nu$ decays via the ''cocktail'' of exclusive modes presented in the Appendix. Monte Carlo simulations show that the $\sin^2\alpha$ distributions for purely semielectronic decays of D^0 mesons and generic decays of D^0 mesons are indistinguishable, and the use of either signal shape (purely semielectronic or generic) results in the same yields. The second order polynomial P^i_2 is also constrained to have the same shape for both the wrong- and right-sign $\sin^2\alpha$ distributions. The yield of $D^0\to Xe^+\nu$ candidates ($N^i_{\rm RS}[D^0\to Xe^+\nu$ or or $D^0\to X\mathcal{F}_e]$), the yield of misidentified hadrons or electrons from $\pi^0\to e^+e^-\gamma$ in the wrong-sign distribution ($b^i_{\rm WS}[D^0\to X\mathcal{F}_e]$), and the normalizations and shape of the background polynomial ($B^i_{\rm RS}$, $B^i_{\rm WS}$ and P^i_2) are determined from the fits to the $\sin^2\alpha$ distribution of the right-sign and wrong-sign samples in bins of pion momentum p_π.

The $\sin^2\alpha$ distributions for the data, with the resulting fits overlaid, are shown in Figs. 2 and 3. Table I presents the right-sign and wrong-sign yields, where the right-sign yields still have a contribution due to $D^0\to X\mathcal{F}_{e^+}$ backgrounds.

IV. DETERMINATION OF THE BACKGROUND CONTRIBUTION TO THE SIGNAL

In this section the magnitude of the misidentified electron background to the right-sign signal yield is determined. Two decay chains contribute to this background: $D^{*+}\to D^0\pi^+$, $D^0\to Xh^+$, where the h^+ is a hadronic track misidentified as an electron, and $D^{*+}\to D^0\pi^+$, $D^0\to X\pi^0$, $\pi^0\to e^+e^-\gamma$. The sum of the right-sign background per pion momentum bin i can be denoted as

$$b^i_{\rm RS}=N^i(\pi^+,X\pi^0)f^i_{e^+}(X\pi^0)+N^i(\pi^+,Xh^+)f^i_{e^+}(Xh^+), \tag{4}$$

where $N^i(\pi^+,X\pi^0)$ [$N^i(\pi^+,Xh^+)$] is the number of inclusive $D^{*+}\to D^0\pi^+$, $D^0\to X\pi^0$ [$D^0\to Xh^+$] decays in the data, and $f^i_{e^+}(X\pi^0)$ [$f^i_{e^+}(Xh^+)$] is the probability for misidentifying this background as signal. We can define the same sum for the wrong-sign yield per pion momentum bin i as

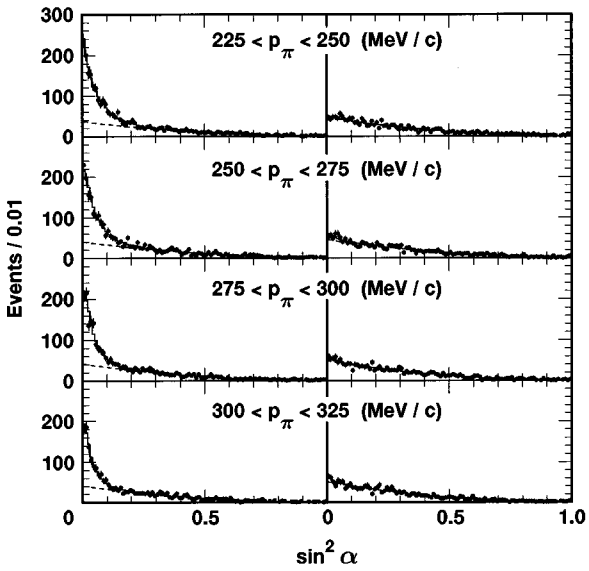

FIG. 2. The $\sin^2\alpha$ distribution for pions with momentum between 225 and 325 MeV/c with an identified electron with $\cos\Theta_{\pi\text{-}e}>0.8$. Events with the electron and pion having the same sign (right sign) are plotted on the left side; the opposite sign events (wrong sign) are plotted on the right side. The points represent the data and the histogram is the result of the fit. The dashed line represents the random pion-electron background and is modeled by a second order polynomial.

$$b^i_{\rm WS}=N^i(\pi^+,X\pi^0)f^i_{e^-}(X\pi^0)+N^i(\pi^+,Xh^-)f^i_{e^-}(Xh^-). \tag{5}$$

The wrong-sign yield and the right-sign background differ only in that positive tracks from D^0 decays are much less

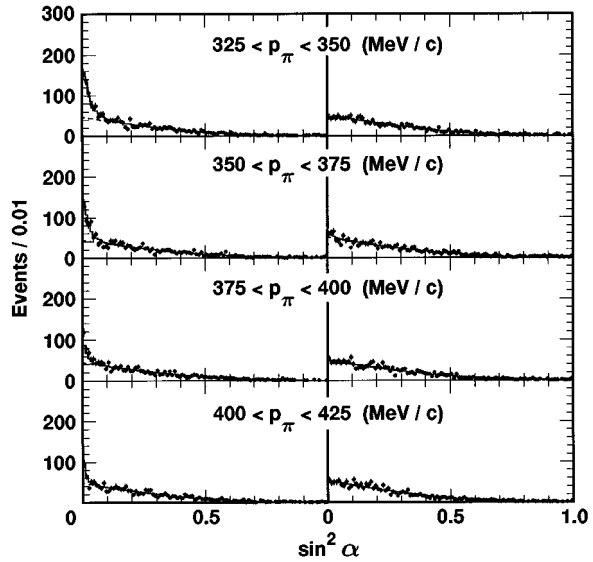

FIG. 3. The $\sin^2\alpha$ distribution for pions with momentum between 325 and 425 MeV/c with an identified electron with $\cos\Theta_{\pi\text{-}e}>0.8$. Events with the electron and pion having the same sign (right sign) are plotted on the left side; the opposite sign events (wrong sign) are plotted between on the right side. The points represent the data and the histogram is the result of the fit. The dashed line represents the random pion-electron background and is modeled by a second order polynomial.

TABLE I. The total yield of candidate $D^{*+}\to D^0\pi^+, D^0\to Xe^+\nu$ events (right sign) and candidate $D^{*+}\to D^0\pi^+, D^0\to Xe^-\nu$ events (wrong sign) as a function of pion momentum. Misidentified electron backgrounds have not yet been subtracted.

$p(\pi)$ (MeV/c)	Yields	
	Right sign	Wrong sign
225–250	1232±53	32±31
250–275	1071±49	74±29
275–300	935±44	45±25
300–325	689±38	39±22
325–350	414±32	−29±18
350–375	259±25	36±17
375–400	166±20	−4±12
400–425	79±15	0±11
Total	4845±104	193±62

likely to be kaons than negative tracks from D^0 decays. Using $f^i_{e^-}(X\pi^0)=f^i_{e^+}(X\pi^0)$, we find

$$b^i_{\rm RS}=b^i_{\rm WS}-N(\pi^+,Xh^-)f^i_{e^-}(Xh^-)+N(\pi^+,Xh^+)f^i_{e^+}(Xh^+). \quad (6)$$

If $N(\pi^+,Xh^+)f^i_{e^+}(Xh^+)=N(\pi^+,Xh^-)f^i_{e^-}(Xh^-)$, then the wrong-sign yield would be equal to the background contribution to the right-sign yield. However, for pions and kaons which pass the same geometry and momentum criteria as the electrons, the π^+:K^+ ratio of h^+ tracks originating from D^0 mesons is quite different from the π^-:K^- ratio. Using world averages [2] of the measured D^0 branching fractions, the π^+:K^+ ratio is 96:4 while the π^-:K^- ratio is 42:58. This difference, coupled with different misidentification rates for pions and kaons, leads to a small correction to the wrong-sign yield.

The probability for a π^+ track to be misidentified as an e^+ is determined by studying a large data sample of $K^0_s\to\pi^+\pi^-$ decays as a function of charged pion momentum. This probability is measured to be (0.056±0.015)% for pions with momentum between 0.7 and 0.9 GeV/c, rising to (0.250±0.059)% for pions with momentum between 1.9 and 2.5 GeV/c. Multiplying this momentum-dependent probability with a Monte Carlo simulation of the π^+ momentum distribution from D^0 and $\overline{D^0}$ decays, we find the misidentification probability, integrated over all pion momenta, to be (0.102±0.016)% for the right-sign pions and (0.093±0.011)% for the wrong-sign pions. These numbers differ due to the different momentum spectra for right-sign and wrong-sign pions. The error is due to the statistical uncertainty in the misidentification probability per track as a function of momentum.

For charged kaons the data do not provide a sample as statistically rich and clean as for pions. The cleanest sample of charged kaons comes from reconstructed $D^0\to K^-\pi^+(\pi^0)$ decays. With 19742±221 reconstructed D^0's with a K^- that passed the momentum cuts, 4.5±5.5 were consistent with the K^- being identified as an electron. This yields a central value of (0.023±0.028)% for the misidentification probability due to kaons. As no momentum dependence measurement is possible we use (0.023±0.028)% as the misidentification probability for charged kaons over the whole momentum range of interest.

Multiplying these misidentification probabilities by the π:K fractions gives the rate per hadronic track from $D^{*+}\to D^0\pi^+$ decays for π^+ momentum between 225 and 425 MeV/c. We obtain a total misidentification probability of $f_{e^+}(\pi^+,Xh^+)=(0.099\pm0.016)\%$ for the right-sign hadronic tracks and $f_{e^-}(\pi^+,Xh^-)=(0.052\pm0.017)\%$ for the wrong-sign hadronic tracks, a difference of a factor of 2. Since the extraction of yields is done in eight 25 MeV/c momentum bins, the probabilities are determined for each of the eight bins individually. Small variations arise due to different D^0 momentum spectra and small changes in the π:K ratio.

To turn these misidentification probabilities into the actual yield of misidentified tracks, the inclusive right-sign and wrong-sign rate [$N(\pi^+,Xh^+)$ and $N(\pi^+,Xh^-)$] is determined from the data. The number of right-sign and wrong-sign hadronic tracks associated with $D^{*+}\to D^0\pi^+$ decays is then determined by using the same code and technique as for identified electrons, without the requirement that the hadronic track be identified as an electron. Table II gives the resulting estimated misidentified charged track contribution to the right- and wrong-sign yields, as well as the final estimated background to the right-sign yield.

TABLE II. Summary of the expected background contribution as a function of pion momentum to the right-sign yield, where $b^i_{\rm RS}=b^i_{\rm WS}-N^i(\pi^+,Xh^-)f^i_{e^-}(Xh^-)+N^i(\pi^+,Xh^+)f^i_{e^+}(Xh^+)$.

$p(\pi)$ (MeV/c)	b^i_{WS}	$N(\pi^+,Xh^-)f^i_{e^-}(Xh^-)$	$N(\pi^+,Xh^+)f^i_{e^+}(Xh^+)$	b^i_{RS}
225–250	32±31	13±3	24±3	43±31
250–275	74±29	13±3	22±3	83±29
275–300	45±25	9±2	17±2	53±25
300–325	39±22	7±2	13±2	45±22
325–350	−29±18	5±1	9±1	−25±18
350–375	36±17	4±1	6±1	38±17
375–400	−4±12	2±1	4±1	−2±12
400–425	0±11	1±1	2±1	1±11
Total	193±62	54±5	97±6	236±64

TABLE III. The yields of inclusive $D^{*+}\to D^0\pi^+$ and $D^0\to Xe^+\nu$ decays, the efficiency for detecting the $Xe^+\nu$ final state, and the calculated branching fraction, as a function of the pion momentum emitted from the D^{*+} decay. The errors are statistical only and include the statistical error on the background subtraction.

$p(\pi)$ (MeV/c)	$N(D^{*+}\to D^0\pi^+)$	$N(D^{*+}\to D^0\pi^+, D^0\to Xe^+\nu)$	$\epsilon(Xe^+\nu)$ (%)	$\mathcal{B}(D^0\to Xe^+\nu)$ (%)
225–250	44161±611	1189±61	37.9	7.10±0.38
250–275	39114±562	988±57	40.1	6.30±0.38
275–300	29482±475	882±51	42.7	7.01±0.42
300–325	21120±396	644±44	43.7	6.97±0.49
325–350	14973±334	439±37	45.5	6.42±0.56
350–375	9165±267	221±30	48.0	5.02±0.70
375–400	5492±208	168±23	49.5	6.18±0.88
400–425	2151±147	78±19	50.7	7.15±1.8
Total	165658±1149	4609±121		6.64±0.18

V. EFFICIENCY

The efficiency for detecting the electron, as determined by the Monte Carlo simulation, depends on the cocktail of exclusive modes used to generate the inclusive semielectronic decays. Table XII in the Appendix presents the ratios of exclusive rates used to calculate the ratios $X_m=\mathcal{B}(D^0\to me^+\nu)/\Sigma_n\mathcal{B}(D^0\to ne^+\nu)$, where $m,n=K^-$, K^{*-}, $K_1^-(1270)$, $K_2^{*-}(1430)$, π^-, and ρ^- mesons. The efficiency for each of these modes is obtained from a Monte Carlo simulation of each individual mode, and the inclusive efficiency is obtained from

$$\epsilon(Xe^+\nu)=\sum_m X_m\epsilon(D^0\to me^+\nu). \tag{7}$$

As in the $D^0\to K^-\pi^+$ analysis, the extraction of yields is done in eight pion momentum bins from 225 to 425 MeV/c. Table III contains the efficiency in each of the eight pion momentum bins, with the efficiencies for the individual exclusive channels in Table XIII (the Appendix). The total systematic error due to uncertainties in the cocktail is determined by varying the ratios in Table XII by one standard deviation, individually and collectively. The largest variation in the overall efficiency is seen when X_K and X_π are both raised or both lowered and the other modes are changed in the opposite direction. This causes a $\pm 2\%$ change in the efficiency and is the estimated systematic error due to the uncertainties in the cocktail of exclusive modes.

In addition to changing the cocktail ratios, the effect of the assumed q^2 dependence of the form factors is studied by changing the Isgur-Scora-Grinstein-Wise (ISGW) slope (κ) [8]. The value used to generate the decays is $\kappa=0.57\pm0.07$, as measured in a large sample of $D^0\to K^-e^+\nu$ decays [4]. Variations of 1σ on κ resulted in a $\pm 0.6\%$ variation in efficiency. The longitudinal and transverse contributions from $D^0\to K^{*-}e^+\nu$ decays were varied by 1σ of their measured value and the total efficiency changed by less than $\pm 0.08\%$ [9].

VI. RESULTS

A. $\mathcal{B}(D^0\to Xe^+\nu)$

Table III shows the relevant measurements for determining $\mathcal{B}(D^0\to Xe^+\nu)$. The first column gives the inclusive $D^{*+}\to D^0\pi^+$ yields from Ref., [3] and the second gives the background subtracted yield of $D^0\to Xe^+\nu$ decays, followed by a column of efficiencies. The last column is the branching fraction for $D^0\to Xe^+\nu$ for the eight momentum bins. As a check that the eight measurements are self-consistent, the χ^2 was calculated under the assumption that all eight branching fraction measurements come from the weighted average. The result is a χ^2 of 9.4 for 7 degrees of freedom.

Sources of systematic effects and their estimated magnitude are listed in Table IV. The dominant systematic uncertainty is the evaluation of the electron identification efficiency. This was studied using an electron identification algorithm developed using radiative Bhabha events. Its performance on continuum events is studied using $\pi^0\to\gamma e^+e^-$ where the e^+e^- pair could originate from either a Dalitz decay of the π^0 or a γ conversion in material. This study resulted in a conservative estimate of the electron identification systematic uncertainty of $\pm 3\%$.

The inclusive semielectronic branching fraction is measured to be

$$\mathcal{B}(D^0\to Xe^+\nu)=[6.64\pm0.18\pm0.29]\%, \tag{8}$$

where the first error is statistical and the second error is the estimated systematic uncertainty. Sources of model dependence have been minimized by relying on the experimental measurements of the exclusive rates of the observed modes

TABLE IV. Estimate of the systematic uncertainty in the measurement of $\mathcal{B}(D^0\to Xe^+\nu)$.

Source	Estimated systematic error (%)
Electron identification efficiency	±3.0
$Xe^+\nu$ cocktail	±2.0
$N(D^{*+})$	±1.5
Track reconstruction	±1.0
Monte Carlo statistics	±1.0
Electron fake rate	±1.0
Form factor slope κ	±0.6
Total	±4.3

TABLE V. The yields of $D\to K^-\pi^+$ decays, the efficiency for detecting the $K^-\pi^+$ final state, the yields of $D^0\to Xe^+\nu$ decays, the efficiency for detecting the $Xe^+\nu$ final state, and the calculated ratio of branching fractions, as a function of the initial D^{*+} pion momentum. The errors on the data yields are statistical only. The error on the ratio of branching fractions is statistical only.

$p(\pi)$ (MeV/c)	$N(D^{*+}\to D^0\pi^+,$ $D^0\to K^-\pi^+)$	$\epsilon(K\pi)$ (%)	$N(D^{*+}\to D^0\pi^+,$ $D^0\to Xe^+\nu)$	$\epsilon(Xe^+\nu)$ (%)	$\frac{\mathcal{B}(D^0\to Xe^+\nu)}{\mathcal{B}(D^0\to K^-\pi^+)}$
225–250	1129±44	64.6	1189±61	37.9	1.80±0.12
250–275	945±40	64.3	988±57	40.1	1.68±0.12
275–300	741±34	64.4	882±51	42.7	1.80±0.13
300–325	528±30	65.1	644±44	43.7	1.82±0.16
325–350	393±25	66.0	439±37	45.5	1.62±0.18
350–375	262±19	66.4	221±30	48.0	1.17±0.18
375–400	153±15	68.8	168±23	49.5	1.53±0.26
400–425	57±9	63.1	78±19	50.7	1.70±0.50
Total	4208±83		4609±121		1.684±0.056

and on experimental measurements of the $d\Gamma/dq^2$ spectrum in $D^0\to K^-e^+\nu$ decays. Models have been used only for the $d\Gamma/dq^2$ spectrum of the other exclusive modes. The previous world average of $[7.01\pm0.62]\%$ is in agreement with this result [2].

B. $\mathcal{B}(D^0\to Xe^+\nu)/\mathcal{B}(D^0\to K^-\pi^+)$

In addition to measuring the absolute $D^0\to Xe^+\nu$ branching fraction, it is straightforward to combine the yields presented here with those in Ref. [3] to obtain a measurement of the ratio $\mathcal{B}(D^0\to Xe^+\nu)/\mathcal{B}(D^0\to K^-\pi^+)$. This is done in Table V, producing a ratio that is independent of systematics associated with the inclusive $D^{*+}\to D^0\pi^+$ yields. Contributions from other sources of systematic errors are given in Table VI. The result is

$$\mathcal{B}(D^0\to Xe^+\nu)/\mathcal{B}(D^0\to K^-\pi^+)=1.684\pm0.056\pm0.093. \tag{9}$$

Again the first error is statistical and the second error is the estimated systematic uncertainty, where the use of a common data set allowed cancellation of some systematic effects present in the individual results.

This ratio provides a check of the ratio

$$X_K=\mathcal{B}(D^0\to K^-e^+\nu)/\mathcal{B}(D^0\to Xe^+\nu) \tag{10}$$

TABLE VI. Estimate of the systematic uncertainty in the measurement of $\mathcal{B}(D^0\to Xe^+\nu)/\mathcal{B}(D^0\to K^-\pi^+)$.

Source	Estimated systematic error (%)
Electron efficiency	±3.0
$Xe^+\nu$ cocktail	±2.0
Track reconstruction	±3.8
Monte Carlo statistics	±1.2
Electron fake rate	±1.0
Form factor slope κ	±0.6
$K^-\pi^+$ (mass fit and momentum cut)	±0.7
Total	±5.5

$$=\frac{\mathcal{B}(D^0\to K^-e^+\nu)}{\mathcal{B}(D^0\to K^-\pi^+)}\frac{\mathcal{B}(D^0\to K^-\pi^+)}{\mathcal{B}(D^0\to Xe^+\nu)}, \tag{11}$$

which is used in the $D^0\to Xe^+\nu$ cocktail. To obtain the most precise value possible, we take advantage of the fact that the CLEO result for $\mathcal{B}(D^0\to K^-e^+\nu)/\mathcal{B}(D^0\to K^-\pi^+)$ was obtained with the same detector. This reduces the systematic bias due to lepton identification (reduced to ±1.7%) and the systematic bias due to tracking reconstruction (reduced to ±2%). There is also a large overlap of $D^0\to K^-\pi^+$ events which were used to calculate the two ratios which appear in Eq. (11) [10]. Using only CLEO results and taking these common systematic effects into account we obtain $X_K=0.581\pm0.023\pm0.028$. Using all measurements of $\mathcal{B}(D^0\to K^-e^+\nu)/\mathcal{B}(D^0\to K^-\pi^+)$ and taking advantage of the common CLEO systematic errors results in a value of $X_K=0.545\pm0.035$ [13]. These results agree well with the input value of X_K listed in Table XII, but are higher than the two measurements by E653, the average of which is $\mathcal{B}(D^0\to K^-\mu^+\nu)/\mathcal{B}(D^0\to X\mu^+\nu)=0.404\pm0.048$ [11,12].

C. Comparison of inclusive measurement to the sum of the exclusive rates

The inclusive semielectronic branching fraction is often compared to the sum of the measured exclusive channels [1,2,16]. This provides an estimate of the fraction of the semielectronic final states that have not yet been identified. In terms of the branching fraction ratios $R_m=\mathcal{B}(D^0\to me^+\nu)/\mathcal{B}(D^0\to K^-e^+\nu)$ (used in the Appendix for tabulating the $D^0\to Xe^+\nu$ cocktail listed in Table XII), the ratio of the difference between the inclusive rate and the sum of the exclusive rates can be written as

$$\frac{\mathcal{B}(D^0\to Xe^+\nu)-\Sigma_m\mathcal{B}(D^0\to me^+\nu)}{\mathcal{B}(D^0\to Xe^+\nu)}$$
$$=1-X_K(1+R_{K*}+R_\pi+R_\rho). \tag{12}$$

Performing the comparison using only CLEO data ($X_K=0.581\pm0.036$ and $1+R_{K*}+R_\pi=1.724\pm0.078$) results in a value of

$$\frac{\mathcal{B}(D^0\to Xe^+\nu)-\Sigma_m\mathcal{B}(D^0\to me^+\nu)}{\mathcal{B}(D^0\to Xe^+\nu)}=(-0.2\pm7.7)\%\,. \tag{13}$$

This CLEO result does not include a contribution from R_ρ as CLEO has not reported a value for this ratio. Inclusion of the small contribution for R_ρ will result in a central value further from zero, while still entirely consistent with zero given the experimental errors. Using the value of $X_K=0.545\pm0.035$ obtained in the previous section and $1+R_{K*}+R_\pi+R_\rho=1.749\pm0.067$ (see Table XII), we find

$$\frac{\mathcal{B}(D^0\to Xe^+\nu)-\Sigma_m\mathcal{B}(D^0\to me^+\nu)}{\mathcal{B}(D^0\to Xe^+\nu)}=(4.7\pm7.5)\%. \tag{14}$$

These results are consistent with the upper limits obtained by direct searches for the unobserved exclusive modes [14].

D. Inclusive electron momentum spectrum

The lepton spectrum from semileptonic charm decays has not been updated since the DELCO results [15]. Because the measurement presented here is not made in the rest frame of the D^0 we compare the observed lepton spectrum in the laboratory frame with that of the Monte Carlo simulation. To obtain the momentum spectrum for inclusive $D^0\to Xe^+\nu$ decays, events were selected that passed all the selection criteria previously described. An additional cut of $\sin^2\alpha<0.12$ is applied. This cut retains 90% of the signal and is large enough that systematics associated with modeling the thrust axis are minimized.

There is still background in this sample whose shape is provided by the wrong-sign candidate electrons. The normalization of this background is obtained by normalizing the wrong-sign $\sin^2\alpha$ distribution to the right-sign $\sin^2\alpha$ distribution for values of $\sin^2\alpha>0.2$. The wrong-sign background correctly models the momentum distribution of random pion-electron combinations and $D^0\to X\pi^0$, $\pi^0\to e^+e^-\gamma$ decays. However, the contribution due to $D^0\to Xh^+$ where h^+ is misidentified as an electron, is underestimated by $[(97-54)0.90=]$ 39 events (see Table II). Also, Monte Carlo simulations show that the momentum spectra are similar but not identical for the right-sign misidentified electrons ($\langle p_{\rm RS}\rangle=1.2$ GeV/c with a rms $=0.58$ GeV/c) and wrong-sign misidentified electrons ($\langle p_{\rm WS}\rangle=1.3$ GeV/c with a rms $=0.64$ GeV/c). The amount of misidentified electron background is less than 1.6% of the total background in the right-sign signal region. Here 56% of this background can be approximately modeled by misidentified electrons in the wrong-sign background. There remains a small amount (0.9% relative to the signal) of unsubtracted misidentified electron background, which we ignore since this test is insensitive to backgrounds at this level.

In Fig. 4 the background-subtracted momentum spectrum for the electrons is shown along with the momentum spectrum obtained from the Monte Carlo simulation. The two distributions are normalized to the same number of events, resulting in a 75% confidence level that the simulation is correctly producing D^{*+} and D^0 mesons and the inclusive $D^0\to Xe^+\nu$ decays. Any deviations would indicate a problem in the simulation, either in the production or decay dynamics. We conclude that the Monte Carlo result provides a good simulation of the data.

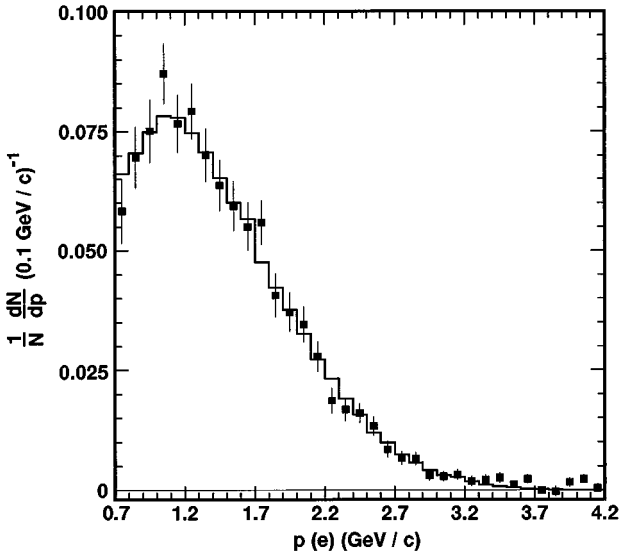

FIG. 4. The laboratory momentum spectrum of electrons from semielectronic D^0 decays. The solid squares represent the background-subtracted data, and the histogram is the result of a Monte Carlo simulation.

VII. CONCLUSIONS

We have presented a new measurement of the inclusive branching fraction for $D^0\to Xe^+\nu$ decays. The final result is

$$\mathcal{B}(D^0\to Xe^+\nu)=[6.64\pm0.18(\text{stat})\pm0.29(\text{syst})]\%. \tag{15}$$

We find that the difference between this inclusive rate and the sum of the observed exclusive channels is $(4.7\pm7.5)\%$ of the inclusive rate. This corresponds to an upper limit on the unobserved modes of 15.6% of the inclusive rate (at the 90% C.L.). The experimental upper limits obtained using direct searches for specific unobserved exclusive semielectronic modes are lower than the limit quoted here. However, the upper limit obtained in this paper is less sensitive to the assumption of what exclusive channels are unobserved. The two methods, direct searches and inclusive-exclusive rate comparison, both suggest that the remaining unobserved exclusive semileptonic modes occur at small rates. In addition the observed electron momentum spectrum from inclusive $D^0\to Xe^+\nu$ decays is seen to be well described by the exclusive semielectronic cocktail.

ACKNOWLEDGMENTS

We gratefully acknowledge the effort of the CESR staff in providing us with excellent luminosity and running conditions. J.P.A., J.R.P., and I.P.J.S. thank the NYI program of the NSF, G.E. thanks the Heisenberg Foundation, K.K.G., M.S., H.N.N., T.S., and H.Y. thank the OJI program of DOE, J.R.P, K.H., and M.S. thank the A.P. Sloan Foundation, and A.W. and R.W. thank the Alexander von Humboldt Stiftung for support. This work was supported by the National Science Foundation, the U.S. Department of Energy, and the

Natural Sciences and Engineering Research Council of Canada.

APPENDIX: DETERMINATION OF THE $D^0 \to X e^+ \nu$ COCKTAIL

In order to calculate the efficiency for observing the electron within the 20° cone around the slow pion direction, the inclusive semielectronic decay was modeled as the sum of many exclusive modes. In this appendix, a list of these exclusive decays and their branching fractions is presented. This list, referred to as the $D^0 \to X e^+ \nu$ cocktail, is determined using world averages to obtain the ratios

$$R_{K^*} = \mathcal{B}(D^0 \to K^{*-} e^+ \nu)/\mathcal{B}(D^0 \to K^- e^+ \nu), \quad \text{(A1)}$$

$$R_\pi = \mathcal{B}(D^0 \to \pi^- e^+ \nu)/\mathcal{B}(D^0 \to K^- e^+ \nu), \quad \text{(A2)}$$

$$R_\rho = \mathcal{B}(D^0 \to \rho^- e^+ \nu)/\mathcal{B}(D^0 \to K^- e^+ \nu). \quad \text{(A3)}$$

Experimental upper limits are used to obtain estimates for the unobserved modes:

$$R_{K(1270)} = \mathcal{B}(D^0 \to K_1^-(1270) e^+ \nu)/\mathcal{B}(D^0 \to K^- e^+ \nu), \quad \text{(A4)}$$

$$R_{K_2^*(1430)} = \mathcal{B}(D^0 \to K_2^{*-}(1430) e^+ \nu)/\mathcal{B}(D^0 \to K^- e^+ \nu). \quad \text{(A5)}$$

The central value used for these unobserved modes is set to half the 90% confidence level upper limit with an error equal to $\pm 100\%$ of the central value.

The ratio X_m of the rate for an exclusive channel $D \to m e \nu$ to the inclusive rate is then obtained from the formulas

$$S = 1 + R_{K^*} + R_\pi + R_\rho + R_{K(1270)} + R_{K_2^*(1430)}, \quad \text{(A6)}$$

$$X_K = 1/S, \quad \text{(A7)}$$

$$X_{K^*} = R_{K^*}/S, \quad \text{(A8)}$$

$$X_\pi = R_\pi/S, \quad \text{(A9)}$$

$$X_\rho = R_\rho/S, \quad \text{(A10)}$$

$$X_{K(1270)} = R_{K(1270)}/S, \quad \text{(A11)}$$

$$X_{K_2^*(1430)} = R_{K_2^*(1430)}/S. \quad \text{(A12)}$$

Throughout this appendix the results are written in terms of the D^0 branching fractions. Results from the D^+ sector are converted into D^0 equivalent branching fractions using isospin and the measured D^0 and D^+ lifetimes. Also semimuonic measurements are converted into semielectronic results by correcting for the phase space difference between the muonic and electronic modes [2]. In several of the tables, two averages are presented, one which includes all the data presented in the table, and another with CLEO results excluded. This is done to avoid double weighting of the CLEO data when performing calculations.

TABLE VII. Direct measurements of the ratio $\mathcal{B}(D \to \overline{K^* e^+ \nu})/\mathcal{B}(D \to \overline{K e^+ \nu})$ and their weighted average.

Experiment	Reference	Mode	$\mathcal{B}(D \to \overline{K^* e^+ \nu})/\mathcal{B}(D \to \overline{K e^+ \nu})$
CLEO, 1993	[4]	D^0 and D^+	0.62 ± 0.08
CLEO, 1991	[18]	D^0	0.51 ± 0.19
Average			0.60 ± 0.07

TABLE VIII. Measurements of the ratio $\mathcal{B}(D^0 \to K^- e^+ \nu)/\mathcal{B}(D^0 \to K^- \pi^+)$ and their weighted average. The average without CLEO measurements is also calculated separately to avoid multiple use of the CLEO results in determining R_{K^*}.

Experiment	Reference	$\mathcal{B}(D^0 \to K^- e^+ \nu)/\mathcal{B}(D^0 \to K^- \pi^+)$
E687, 1994	[17]	0.878 ± 0.045
CLEO, 1993	[4]	0.978 ± 0.052
CLEO, 1991	[18]	0.86 ± 0.07
E691	[19]	0.91 ± 0.13
E687, 1990	[20]	0.84 ± 0.19
Average without CLEO		0.874 ± 0.035
Average		0.908 ± 0.029

1. $R_{K^*} = \mathcal{B}(D^0 \to K^{*-} e^+ \nu)/\mathcal{B}(D^0 \to K^- e^+ \nu)$

There are two methods to measure this ratio: direct and indirect. The direct measurements, given in Table VII, can only be performed when both the K and K^* modes are reconstructed through the same parent species within the same experiment. The indirect measurement compares the $K^{*0} e^+ \nu$ width measured in D^+ decays to the $K^- e^+ \nu$ width measured in D^0 decays, via

$$R_{K^*}^{\text{indirect}} = \frac{\mathcal{B}(D^+ \to \overline{K^{*0}} e^+ \nu)}{\mathcal{B}(D^+ \to K^- \pi^+ \pi^+)} \frac{\mathcal{B}(D^0 \to K^- \pi^+)}{\mathcal{B}(D^0 \to K^- e^+ \nu)} \times \frac{\mathcal{B}(D^+ \to K^- \pi^+ \pi^+)}{\mathcal{B}(D^0 \to K^- \pi^+)} \frac{\tau_{D^0}}{\tau_{D^+}}. \quad \text{(A13)}$$

Table VIII contains the world average for $\mathcal{B}(D^0 \to K^- e^+ \nu)/\mathcal{B}(D^0 \to K^- \pi^+)$ and Table IX contains the

TABLE IX. Measurements of the ratio $\mathcal{B}(D^+ \to \overline{K^{*0}} e^+ \nu)/\mathcal{B}(D^+ \to K^- \pi^+ \pi^+)$ and their weighted average.

Experiment	Reference	$\mathcal{B}(D^+ \to \overline{K^{*0}} e^+ \nu)/\mathcal{B}(D^+ \to K^- \pi^+ \pi^+)$
E691	[21]	0.49 ± 0.06
E687	[22]	0.59 ± 0.07
CLEO	[4]	0.67 ± 0.11
E653	[23]	0.48 ± 0.11
Argus	[24]	0.55 ± 0.13
WA82	[25]	0.62 ± 0.17
Average	without CLEO	0.527 ± 0.041
Average		0.547 ± 0.038

TABLE X. Measurements of the hadronic normalizing modes $D^0\to K^-\pi^+$, $D^+\to K^-\pi^+\pi^+$, and their ratio. The CLEO result on $\mathcal{B}(D^+\to K^-\pi^+\pi^+)/\mathcal{B}(D^0\to K^-\pi^+)$ is a direct measurement of this ratio, and is not obtained by dividing the individual CLEO results.

Experiment	Reference	$\mathcal{B}(D^0\to K^-\pi^+)$ (%)	$\mathcal{B}(D^+\to K^-\pi^+\pi^+)$ (%)	$\frac{\mathcal{B}(D^+\to K^-\pi^+\pi^+)}{\mathcal{B}(D^0\to K^-\pi^+)}$
CLEO	[3]	3.91 ± 0.19	9.3 ± 1.0	2.35 ± 0.23
ARGUS	[26]	3.41 ± 0.30		
ALEPH	[27]	3.89 ± 0.33		
Mark III	[28]	4.2 ± 0.6	9.1 ± 1.4	
Mark II	[29]	4.1 ± 0.6	9.1 ± 1.9	
ARGUS	[30]	4.5 ± 0.7		
HRS	[31]	4.50 ± 0.94		
Mark I	[32]	4.3 ± 1.0	8.6 ± 2.0	
Average	without CLEO	3.84 ± 0.18	8.98 ± 0.98	2.34 ± 0.28
Average		3.87 ± 0.13	9.1 ± 0.7	2.35 ± 0.18

world average for $\mathcal{B}(D^+\to\overline{K^{*0}}e^+\nu)/\mathcal{B}(D^+\to K^-\pi^+\pi^+)$ where the CLEO measurements have been specifically excluded as these measurements are used in the direct determination of R_{K^*}. To determine $R_{K^*}^{\rm indirect}$, the ratio of normalizing modes $K\pi\pi/K\pi$ presented in Table X is used. Using the world average for this ratio of branching fractions and the D^+/D^0 lifetime ratio [2] the value for $R_{K^*}^{\rm indirect}$ is measured to be 0.556 ± 0.066. Averaging $R_{K^*}^{\rm direct}$ and $R_{K^*}^{\rm indirect}$ yields

$$R_{K^*}=0.577\pm0.048. \tag{A14}$$

2. $R_\pi=\mathcal{B}(D^0\to\pi^-e^+\nu)/(D^0\to K^-e^+\nu)$

The Cabibbo-suppressed decay $D^0\to\pi^-e^+\nu$ has been observed at Mark III. CLEO has made measurements of both the $D^0\to\pi^-e^+\nu$ as well as the $D^+\to\pi^0e^+\nu$ decay chain. There is factor of 2 due to isospin that is needed to convert the $D^+\to\pi^0e^+\nu$ measurement to a $D^0\to\pi^-e^+\nu$ branching fraction. The results are presented in Table XI.

3. $R_\rho=\mathcal{B}(D^0\to\rho^-e^+\nu)/\mathcal{B}(D^0\to K^-e^+\nu)$

Fermilab experiment E653 has published an observation of four $D^+\to\rho^0\mu^+\nu$ events based on a kinematic separation of the Cabibbo-suppressed $\rho^0\mu^+\nu$ signal from the more copious $\overline{K^{*0}}\mu^+\nu$ mode [36]. They measure $\mathcal{B}(D^+\to\rho^0\mu^+\nu)/\mathcal{B}(D^+\to\overline{K^{*0}}\mu^+\nu)=0.044^{+0.032}_{-0.025}\pm0.014$. To obtain R_ρ this measurement needs be corrected by the isospin factor and multiplied by R_{K^*} which gives $R_\rho=\mathcal{B}(D^+\to\rho^0\mu^+\nu)/\mathcal{B}(D^+\to\overline{K^{*0}}\mu^+\nu)\times R_{K^*}\times I_\rho=(0.044^{+0.031}_{-0.025}\pm0.014)(0.579\pm0.049)\times2=0.051\pm0.037$. For Monte Carlo generation it is assumed that the form factor ratios for $D^0\to\rho^-e^+\nu$ decay are identical to those of the well measured $D^0\to K^{*-}e^+\nu$ decay.

TABLE XI. Measurements of the ratio $\mathcal{B}(D^0\to\pi^-e^+\nu)/\mathcal{B}(D^0\to K^-e^+\nu)$ ratio and their weighted average.

Experiment	Reference	Mode	$\mathcal{B}(D^0\to\pi^-e^+\nu)/\mathcal{B}(D^0\to K^-e^+\nu)$
CLEO	[33]	$\pi^-e^+\nu$	0.103 ± 0.041
Mark III	[34]	$\pi^-e^+\nu$	0.115 ± 0.051
CLEO	[35]	$\pi^0e^+\nu$	0.17 ± 0.06
Average			0.121 ± 0.028

4. $\mathcal{B}(D^0\to(\overline{K^*}\pi)^-e^+\nu)$ upper limits

Searches for higher $K^{(*)}$ resonances and possible nonresonant contributions to D semileptonic decay have been performed by the fixed target experiments [14]. Although no evidence for these decays has been demonstrated we include $D^0\to K^-(1270)e^+\nu$ and $D^0\to K_2^{*-}(1430)e^+\nu$ in the Monte Carlo simulation. The decays are generated unpolarized and with the following strengths and errors: $R_{K(1270)}=\mathcal{B}(D^0\to K_1^-(1270)e^+\nu)\,/\,\mathcal{B}(D^0\to K^-e^+\nu)=0.03\pm0.03$ and $R_{K_2^*(1430)}=\mathcal{B}(D^0\to K_2^{*-}(1430)e^+\nu)/\mathcal{B}(D^0\to K^-e^+\nu)=0.02\pm0.02$. It is assumed that any nonresonant contribution to the inclusive rate will have a similar electron momentum spectrum distribution as these higher order modes.

5. Calculation of the $D^0\to Xe^+\nu$ cocktail

Table XII summarizes the relative rates R_m (relative to $D^0\to K^-e^+\nu$) obtained in the previous sections. The sum of these rates is then used to determine the ratio of each exclu-

TABLE XII. The world average or estimate of the ratio of exclusive channels relative to the $D^0\to K^-e^+\nu$ decay mode, $R_m=\mathcal{B}(D^0\to me^+\nu)/\mathcal{B}(D^0\to K^-e^+\nu)$. The third column is the ratio of the exclusive rate to the sum of the exclusive rates, $X_m=\mathcal{B}(D^0\to me^+\nu)/\Sigma_m R_m$.

Mode	R_m	X_m
$D^0\to K^-e^+\nu$	1.0	0.556 ± 0.023
$D^0\to K^{*-}e^+\nu$	0.577 ± 0.048	0.321 ± 0.021
$D^0\to\pi^-e^+\nu$	0.121 ± 0.028	0.067 ± 0.015
$D^0\to\rho^-e^+\nu$	0.051 ± 0.037	0.028 ± 0.020
$D^0\to K_1^-(1270)e^+\nu$	0.03 ± 0.03	0.017 ± 0.016
$D^0\to K_2^{*-}(1430)e^+\nu$	0.02 ± 0.02	0.011 ± 0.011
Sum	1.799 ± 0.076	

TABLE XIII. Efficiencies for the exclusive decay channels used in the $Xe^+\nu$ cocktail.

$p(\pi)$ MeV/c	$\epsilon(K^-e^+\nu)$ (%)	$\epsilon(K^{*-}e^+\nu)$ (%)	$\epsilon(\pi^-e^+\nu)$ (%)	$\epsilon(\rho^-e^+\nu)$ (%)	$\epsilon(K_1^-(1270)e^+\nu)$ (%)	$\epsilon(K_2^{*-}(1430)e^+\nu)$ (%)
225–250	40.4	34.4	42.4	38.1	20.4	10.9
250–275	42.8	36.3	45.4	39.5	22.9	11.7
275–300	45.6	38.6	47.6	42.6	20.6	12.0
300–325	46.2	40.4	49.2	43.8	23.4	13.0
325–350	48.6	41.0	51.0	46.6	27.2	12.0
350–375	50.8	44.1	54.6	43.7	30.7	14.6
375–400	51.9	46.1	56.6	48.2	29.4	19.5
400–425	53.9	45.2	57.7	57.4	21.4	34.3

sive rate to the sum of all the exclusive rates as per Eqs. (A6)–(A12). Table XIII contains the efficiencies for these exclusive modes to pass the selection criteria.

6. Comparison of the inclusive rate to the sum of the exclusive measurements

One of the most frequent comparisons in the literature [1,2,16] is the sum of the observed exclusive channels to the measured inclusive rate. The method of comparing the inclusive measurement to the sum of the ratio of exclusive measurements is presented here.

The following set of equations are used to calculate the branching fraction for the observed exclusive decays:

$$\mathcal{B}(D^0\to K^-e^+\nu)=r_{K\pi}^{Ke^+\nu}\times\mathcal{B}(D^0\to K^-\pi^+), \quad \text{(A15)}$$

$$\mathcal{B}(D^0\to K^{*-}e^+\nu)=r_{K\pi}^{Ke^+\nu}\times\mathcal{B}(D^0\to K^-\pi^+)\times R_{K^*}, \quad \text{(A16)}$$

$$\mathcal{B}(D^0\to \pi^-e^+\nu)=r_{K\pi}^{Ke^+\nu}\times\mathcal{B}(D^0\to K^-\pi^+)\times R_{\pi}, \quad \text{(A17)}$$

$$\mathcal{B}(D^0\to \rho^-e^+\nu)=r_{K\pi}^{Ke^+\nu}\times\mathcal{B}(D^0\to K^-\pi^+)\times R_{\rho}. \quad \text{(A18)}$$

The sum of the observed exclusive rates is then

$$\sum_m \mathcal{B}(D^0\to me^+\nu)=r_{K\pi}^{Ke^+\nu}\times\mathcal{B}(D^0\to K^-\pi^+)\times(1+R_{K^*}+R_{\pi}+R_{\rho}). \quad \text{(A19)}$$

The quantities $r_{K\pi}^{Ke^+\nu}=\mathcal{B}(D^0\to K^-e^+\nu)/\mathcal{B}(D^0\to K^-\pi^+)$ and $\mathcal{B}(D^0\to K^-\pi^+)$ are common to all derived exclusive branching fractions, and thereby affect the entire scale. Dividing Eq. (A19) by $\mathcal{B}(D^0\to Xe^-\nu)$ allows the difference between the inclusive rate and the sum of the exclusive rates relative to the inclusive rate to be obtained without explicitly calculating the rate of the exclusive modes, as per Eq. (12).

[1] Jeffery D. Richman and Patricia R. Burchat, Rev. Mod. Phys. **67**, 893 (1995). In this review of charm and beauty semileptonic decays, they obtain a value for the difference between the inclusive rate and the exclusive rate of $(16\pm5)\%$ of the inclusive rate.

[2] L. Montanet *et al.*, Particle Data Group, Phys. Rev. D **50**, 1173 (1994). Within the *Note on Semileptonic Decays of D and B Mesons, Part I* by R. J. Morrison and J. D. Richman, they obtain a value for the difference between the inclusive rate and the exclusive rate of $(18\pm8)\%$ of the inclusive rate.

[3] CLEO Collaboration, D. S. Akerib *et al.*, Phys. Rev. Lett. **71**, 3070 (1993).

[4] CLEO Collaboration, A. Bean *et al.*, Phys. Lett. B **317**, 647 (1993).

[5] CLEO Collaboration, Y. Kubota *et al.*, Nucl. Instrum. Methods **320**, 66 (1992).

[6] Charge conjugation is implied throughout this paper. The word electron will be used to refer to both e^-'s and e^+'s.

[7] Other sources of right- and wrong-sign electrons are D^0-$\overline{D^0}$ mixing and flavor-changing neutral currents, $D^0\to e^+e^-$. Experimental limits and theoretical expectations on these rare processes make their contribution to the right- and wrong-sign yields negligible [2].

[8] N. Isgur, D. Scora, B. Grinstein, and M. B. Wise, Phys. Rev. D **39**, 799 (1989).

[9] The $D\to\overline{K^*}e^+\nu$ decay has three helicity states in the limit of negligible lepton mass. In Monte Carlo generation the world average [21–23] of the three form factors involved in the decay is used to determine the ratio of longitudinal to transverse alignments ($\Gamma_L/\Gamma_T=1.23\pm0.13$).

[10] When combining the CLEO result for $\mathcal{B}(D^0\to K^-e^+\nu)/\mathcal{B}(D^0\to K^-\pi^+)$ and the CLEO result for $\mathcal{B}(D^0\to Xe^+\nu)/\mathcal{B}(D^0\to K^-\pi^+)$ we use the following values which have reduced systematic errors as explained in the text: $\mathcal{B}(D^0\to K^-e^+\nu)/\mathcal{B}(D^0\to K^-\pi^+)=0.978\pm0.025\pm0.032$, $\mathcal{B}(D^0\to Xe^+\nu)/\mathcal{B}(D^0\to K^-\pi^+)=1.684\pm0.049\pm0.061$.

[11] E653 Collaboration, K. Kodama *et al.*, Phys. Rev. Lett. **66**, 1819 (1991).

[12] E653 Collaboration, K. Kodama *et al.*, Phys. Lett. B **336**, 605 (1994).

[13] This value for X_K includes the CLEO and non-CLEO results for $R=\mathcal{B}(D^0\to K^-e^+\nu)/\mathcal{B}(D^0\to K^-\pi^+)$. The weighted average of $R(\text{CLEO})=0.978\pm0.041$ (from [10]) and $R(\text{non}-\text{CLEO})=0.874\pm0.035$ is $R(\text{wtd})=0.918\pm0.027$. To calculate X_K one divides by the branching fraction ratio

$R' = \mathcal{B}(D^0 \to X e^+ \nu)/(D^0 \to K^- \pi^+)$. Using only CLEO data to calculate X_K, the statistical and systematic errors of R and R' are reduced because of the cancellation of the contributions from $\mathcal{B}(D^0 \to K^- \pi^+)$, and one calculates $X_K = R/R' = (0.978 \pm 0.041)/(1.684 \pm 0.078) = 0.581 \pm 0.036$, where R and R' are taken from [10]. Using R(non-CLEO) to calculate X_K, one obtains $X_K = R/R' = (0.874 \pm 0.035)/(1.684 \pm 0.109) = 0.519 \pm 0.040$. In this case the full errors for R' are used [see Eq. (9)], because the non-CLEO measurement of R has no experimental correlation with the CLEO measurement of R'. To combine the CLEO and non-CLEO results for R to calculate X_K, one needs a weighted value of R' from the two values given above. $R'(\text{wtd}) = 1.684 \pm [0.078 f(\text{correlated}) + 0.109 f(\text{uncorrelated})]$, where $f(\text{uncorrelated}) = 1 - f(\text{correlated}) = (1/0.035)^2/[(1/0.035)^2 + (1/0.041)^2] = 0.578$. This results in $R'(\text{wtd}) = 1.684 \pm 0.096$. Taking the ratio $R(\text{wtd})/R'(\text{wtd}) = (0.918 \pm 0.027)/(1.684 \pm 0.096)$ one calculates $X_K = 0.545 \pm 0.035$.

[14] E653 Collaboration, K. Kodama *et al.*, Phys. Lett. B **313**, 260 (1993); E687 Collaboration, P. L. Frabetti *et al.*, *ibid.* **307**, 262 (1993).

[15] DELCO Collaboration, W. Bacino *et al.*, Phys. Rev. Lett. **43**, 1073 (1979).

[16] M. Witherell, in *Lepton and Photon Interactions*, Proceedings of the 16th International Symposium, Ithaca, New York, 1993, edited by P. Drell and D. Rubin, AIP Conf. Proc. No. 302 (AIP, New York, 1994); John Cumalat, in *The Fermilab Meeting*, Proceedings of the 7th Meeting of the Division of Particles and Fields of the APS, Batavia, Illinois, 1992, edited by C. Albright *et al.* (World Scientific, Singapore, 1993); D. M. Potter, in *Proceedings of the Joint International Lepton-Photon Symposium and Europhysics Conference on High Energy Physics*, Geneva, Switzerland, 1991, edited by S. Hegarty, K. Potter, and E. Quercigh (World Scientific, Singapore, 1992).

[17] E687 Collaboration, P. L. Frabetti *et al.*, Phys. Lett. B **364**, 127 (1995).

[18] CLEO Collaboration, G. Crawford *et al.*, Phys. Rev. D **44**, 3394 (1991).

[19] E691 Collaboration, J. C. Anjos *et al.*, Phys. Rev. Lett. **62**, 1587 (1989).

[20] E687 Collaboration, P. L. Frabetti *et al.*, Phys. Lett. B **315**, 203 (1992).

[21] E691 Collaboration, J. C. Anjos *et al.*, Phys. Rev. Lett. **65**, 2630 (1990).

[22] E687 Collaboration, P. L. Frabetti *et al.*, Phys. Lett. B **307**, 262 (1993).

[23] E653 Collaboration, K. Kodama *et al.*, Phys. Lett. B **286**, 187 (1992).

[24] ARGUS Collaboration, H. Albrecht *et al.*, Phys. Lett. B **255**, 634 (1991).

[25] WA82 Collaboration, M. Adamovich *et al.*, Phys. Lett. B **268**, 142 (1991).

[26] ARGUS Collaboration, H. Albrecht *et al.*, Phys. Lett. B **340**, 125 (1994).

[27] The updated ALEPH result can be found in P. Burchat, ''Review of Charm Physics,'' Report No. SCIPP-93-44 (unpublished). The original ALEPH result can be found in D. Decamp *et al.*, Phys. Lett. B **266**, 218 (1991).

[28] Mark III Collaboration, J. Adler *et al.*, Phys. Rev. Lett. **60**, 89 (1988).

[29] Mark II Collaboration, R. H. Schindler *et al.*, Phys. Rev. D **24**, 78 (1981).

[30] ARGUS Collaboration, H. Albrecht *et al.*, Phys. Lett. B **324**, 249 (1994).

[31] HRS Collaboration, S. Abachi *et al.*, Phys. Lett. B **205**, 411 (1988).

[32] Mark I Collaboration, I. Peruzzi *et al.*, Phys. Rev. Lett. **39**, 1301 (1977).

[33] CLEO Collaboration, F. Butler *et al.*, Phys. Rev. D **52**, 2656 (1995).

[34] Mark III Collaboration, J. Adler *et al.*, Phys. Rev. Lett. **62**, 1821 (1989).

[35] CLEO Collaboration, M. S. Alam *et al.*, Phys. Rev. Lett. **71**, 1311 (1993).

[36] E653 Collaboration, K. Kodama *et al.*, Phys. Lett. B **316**, 455 (1993).